2.26 Mitigation of Collective Effects by Optics Optimization

F. Antoniou, H. Bartosik, Y. Papaphilippou
CERN, 1211 Geneva 23, Switzerland
Mail to: Yannis.Papaphilippou@cern.ch

2.26.1 Introduction

The quantities characterizing the performance of a large variety of hadron and lepton rings, as the power of synchrotron based proton drivers, the luminosity of colliders, the brightness of their associated injectors or the brilliance of X-ray storage rings, are proportional to the beam intensity or to the ratio of the intensity with the beam dimensions. The modern tendency is to push the performance frontiers towards extreme conditions, i.e. the highest beam intensity contained within the smallest beam volume, where the collective behavior of the beam becomes predominant. It is thus of paramount importance to take measures in order to alleviate collective effects, including instabilities, space-charge and intrabeam scattering (IBS), in the early phase of the design, which usually begins with the linear optics.

In the case of rings in operation, dealing with collective effects usually implicates mitigation techniques based on the use of multipole magnets [1] or higher harmonic RF cavities [2] for providing Landau damping, dedicated feedback systems [3] or the reduction of the beam interaction with its environment through careful vacuum and low-impedance component design [4]. Changing the linear optics, without major upgrade involving radical modifications of the machine configuration, is an unconventional approach, since it is subject to the constraints of the existing magnet and powering systems. It can be even more challenging because of its interplay with the already optimized operation of critical systems, such as beam transfer elements or RF. On the other hand, if a viable solution is found, it can be a very cost effective way to break existing intensity or brightness limits.

2.26.2 Impact of Optics Parameters on Collective Effects

In this section, three fundamental quantities that affect collective effects are described, following the logical route of an optics study: starting from the most basic one, the beam energy, passing to the most fundamental, the transverse beam sizes and ending with the phase slip factor, the most intimately connected to collective effects.

The beam energy is one among the basic parameters that have to be settled even before starting the optics design of a ring. Although, strictly speaking, it cannot be considered as an optics constraint, it is indirectly related through the integrated magnet strengths and the size of the lattice cells. At the same time, in the absence of synchrotron radiation damping, the transverse emittance is inversely proportional to the energy, thus reducing the physical beam size. Almost all collective effects become less pronounced with the beam energy, with the notable exception of the electron cloud instability thresholds [5]. Hence, for hadron rings, it is natural to target always the highest possible energy although this heavily depends on the users' physics needs, the reach of the pre-injectors and finally on cost. In the case of beams dominated by synchrotron radiation damping, the quadratic dependence of the horizontal equilibrium emittance to the energy puts an additional restriction to this increase, and a careful optimization has to be performed, in order to meet the specific design targets.

Transverse beam sizes are also playing an important role to the collective beam behavior, especially in the case of self-induced fields. For example, the space-charge tune-shift [6] and IBS growth rates [7] are inversely proportional to their product raised to a certain power. For high-intensity/power rings, there is usually no specific preference on the size of transverse emittances and the trend is to produce them large enough, for limiting the aforementioned effects. When the performance target is high brightness, which corresponds to small transverse emittances, the optics is one handle to increase beam sizes. For hadron rings, the FODO cells are well suited for this, due to the alternating behavior of the optics functions. In particular, weaker focusing can maximize beam sizes, within the limits set by the machine aperture. In the case of e^+/e^- rings targeting low emittances, doublet-like cells are usually employed for minimizing horizontal beam sizes. On the other hand, the vertical beta functions can be increased, especially along the bending magnets, where the horizontal ones are small. Although this strategy is valid for space-charge or IBS, beam current thresholds of instabilities such as transverse mode coupling or coupled bunch, present an opposite dependence and call for a reduction of the average (vertical) beta functions.

The slippage (or phase slip) factor η is defined as the rate of change of the revolution frequency with the momentum deviation. At leading order, it is a function of the relativistic γ factor (i.e. the energy) and the momentum compaction factor α_p:

$$\eta = \alpha_p - \frac{1}{\gamma^2}. \tag{1}$$

The momentum compaction factor is the rate of change of the circumference C with the momentum spread and, again at leading order, it is given by

$$\alpha_p = \frac{1}{C}\oint \frac{D_x(s)}{\rho(s)} ds. \tag{2}$$

It depends on the variation of the horizontal dispersion function along the bending magnets. The phase slip factor unites transverse and longitudinal particle motion. In fact, the synchrotron frequency or the bunch length are proportional to $\eta^{1/2}$, which means that increasing the slippage factor makes synchrotron motion faster.

The phase slip factor vanishes when $\gamma = \alpha_p^{-1/2} = \gamma_t$ and the corresponding energy is named transition energy. It is widely known, since the commissioning of the first synchrotrons, that crossing transition can cause various harmful effects with respect to the collective behavior of the beam [8], as the longitudinal motion basically freezes at this point. Although several transition crossing schemes have been proposed and operated reliably in synchrotrons like the CERN PS for more than 40 years (see [9] and references therein), the call for beams with higher intensity (or power) resulted in the consideration of ring designs which avoid transition, either by injecting above (η>0), or always remaining below transition (η<0). The former case is almost always true for electron/positron rings above a few hundred MeV (unless α_p<0). For hadron rings, it requires the combination of high energy (i.e. large circumference) and a large momentum compaction, which is translated to larger dispersion excursions and, generally speaking, weaker focusing, thereby larger beam sizes [10]. For remaining below transition, the operating energy range has to be kept narrow and a positive momentum compaction factor should be low, which points towards stronger focusing and smaller beam sizes. The special case of negative momentum compaction

(NMC) [11] is very interesting because the beam remains below transition independent of energy. As for the rings remaining above transition, the need to excite dispersion oscillations for getting an overall negative dispersion integral on the bends results in larger beam sizes.

2.26.3 **High-Power Synchrotrons**

Recent optics design of high-intensity and/or high-power rings such as the J-Parc main ring [12], the PS2 [13], or the High-Power PS [14] are based on NMC arc cells, for avoiding transition and reducing losses. These are sequences of modified FODO cells with an increased number of quadrupole families (up to four) for inducing negative dispersion, leading to an overall “imaginary” γ_t [11]. In that case, the absolute value of the slippage factor could be increased for raising instability thresholds but also because a fast synchrotron frequency would be beneficial for longitudinal beam manipulation [15]. A complete picture of the achievable tuning range of a ring such as the PS2 can be obtained by the Global Analysis of all Stable Solutions (GLASS), a numerical method pioneered in low emittance rings [17], where all possible quadrupole configurations providing stable solutions are obtained. In Fig. 1 (left), the imaginary transition γ_t is presented for all stable solutions in the tune diagram, along with resonance lines up to 3rd order. The blue zones corresponding to low imaginary values of γ_t (i.e. large absolute values of the momentum compaction) are obtained for higher horizontal tunes. There is large flexibility for the vertical tunes. In Fig. 1 (right), the geometrical acceptance is computed for the most demanding beam parameters with respect to emittance. The red color corresponds to small acceptance (above a limit of 3.5σ), which means larger beam sizes. This type of global analysis including non-linear dynamics constraints was used during the conceptual design of the PS2 ring [16].

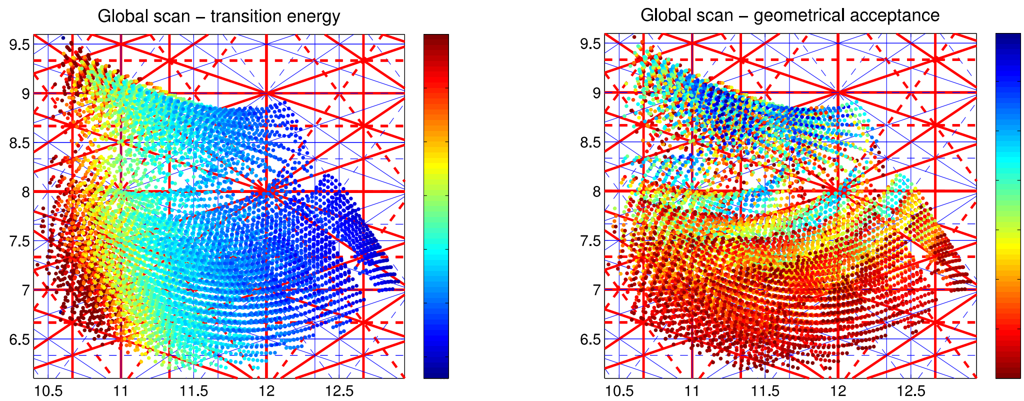

Figure 1: Transition energy γ_t (left) and geometrical acceptance in units of beam sizes $N\sigma$ (right) for a global scan of optics solutions in the tune diagram [17].

2.26.4 **Low Emittance Rings**

The present trend of ultra-low emittance rings is to target the highest beam intensities within the smallest dimensions, at least in the transverse plane. The additional complication in the case of damping rings (DRs) for linear colliders is that they aim to produce low longitudinal emittances, as well. The output beam dimensions are largely dominated by IBS.

Even space-charge effects become important, especially in the vertical plane. A careful optimization of the optics parameters is crucial for reducing these effects and obtaining a solid conceptual design [19].

Due to the fact that the IBS growth rates but also the equilibrium emittances vary with energy, it is important to find their interdependence, when the IBS effect is included [20]. Evaluated through a modified version of the Piwinski method [21], and for constant longitudinal emittance, the dependence of the steady state transverse emittances of the CLIC DRs on the energy is plotted in Fig. 2 (left). A broad minimum is observed around 2.6 GeV for both horizontal (blue) and vertical planes (green). The IBS effect becomes weaker with the increase of energy, as shown in Fig. 2 (right), where the emittance blow-up for all beam dimensions is presented. Although higher energies may be desirable for reducing further collective effects, the output emittance is increased above the target value, due to the domination of quantum excitation. In this respect, it was decided to increase the CLIC DR energy to 2.86 GeV, already reducing the IBS impact by a factor of two, as compared to earlier designs at 2.42 GeV [20].

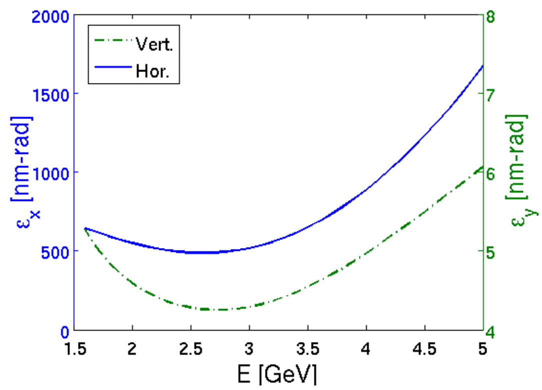

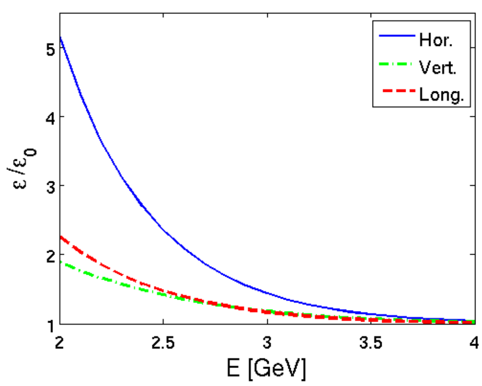

Figure 2: Steady-state emittances (left) and their blow-up (right) due to IBS, as a function of the energy [19].

In modern low emittance rings, Theoretical Minimum Emittance (TME) arc cells or multi bend achromats are employed. In order to reach minimum emittance, the horizontal beam optics is quite constrained, whereas the vertical one is free, but also completely determined by the two quadrupole families of the cell. It turns out that the vertical beta function reaches a minimum at the same location as the horizontal, which is the worst case for IBS. A way to reverse this tendency is to use a combined function dipole with a low defocusing gradient. Although this gradient does not provide a significant effect to the emittance reduction, it reverses the behavior of the vertical beta function at the middle of the dipole, maximizing the vertical beam size at that location, and thus reducing IBS growth rates [22].

A crucial step in the optimization of the TME cell with respect to its impact on collective effects is the analytical derivation of the two quadrupole focal lengths, in thin lens approximation, depending only on the horizontal optics functions at the center of the dipole and the drift space lengths [19, 23]. Using this representation, the dependence of various parameters on the cell phase advances in the case of the CLIC DRs are presented in Fig. 3, including the average IBS growth rates, the detuning from the minimum emittance, the momentum compaction factor, the vertical space-charge tune-shift and the horizontal chromaticity. This parameterization permitted to find the best compromise for the phase advances (between 0.4 and 0.5) where the IBS growth rates, the horizontal and vertical chromaticities and the Laslett tune shift are minimized, while the momentum compaction factor is maximized. These low phase advances correspond to emittances that deviate from the absolute minimum by a factor of around 15. A similar study was performed in order to find the optimal wiggler field and wavelength, while minimizing the IBS effect [19, 24]. Based on these studies, the highest field within the limit of technology would be desirable, but a moderate wavelength is necessary for reducing IBS. These specifications were used for the super-conducting wiggler prototype under development for the CLIC DRs [24].

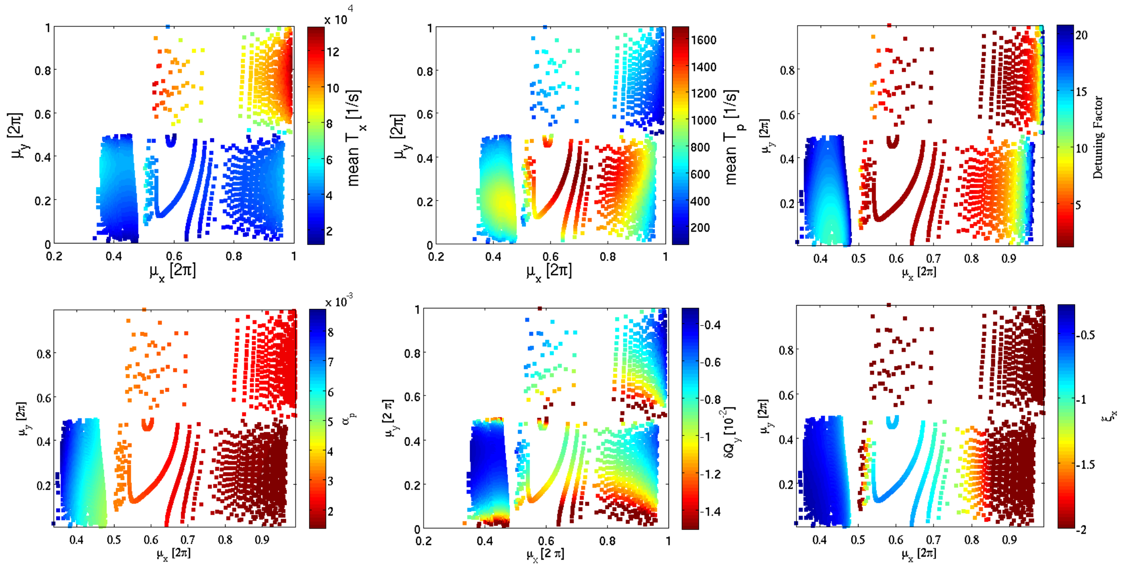

Figure 3: Analytical parameterization of the TME cell phase advances with the IBS horizontal (top, left) and longitudinal (top, middle) growth rates, the detuning factor (top, right), the momentum compaction factor (bottom, left), the Laslett tune shift (bottom, middle) and the horizontal chromaticity (bottom, right) [19].

2.26.5 **High-Brightness Synchrotrons**

Hadron collider injectors need to achieve the highest brightness with the smallest possible losses. A typical example is the CERN SPS whose performance limitations and their mitigations for LHC beams are the subject of a study group [25], in view of reaching the required beam parameters for the high luminosity LHC (HL-LHC). The upgrade of the main 200 MHz RF system will solve beam loading issues for reaching higher intensities, but a variety of single and multi-bunch instabilities remain to be confronted. The Transverse Mode Coupling Instability (TMCI) in the vertical plane and E-Cloud Instability (ECI) for 25 ns beams are the most prominent transverse problems, especially for HL-LHC intensities. Longitudinal instabilities necessitate the use of a higher harmonic 800 MHz RF system for providing Landau damping and the application of controlled longitudinal emittance blow-up throughout the ramp. For constant longitudinal bunch parameters and matched RF-voltage, higher intensity thresholds for the above instabilities are expected when increasing the phase slip factor.

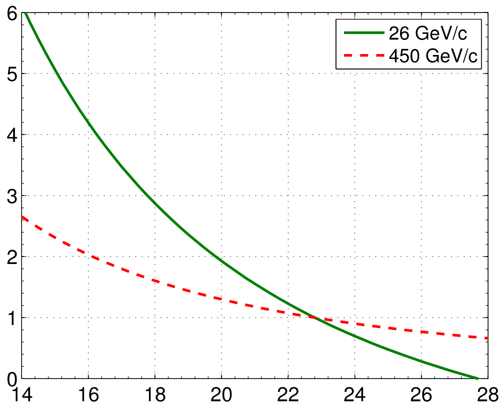

Figure 4: Slippage factor η relative to the value of the nominal SPS optics (nominal γ_t = 22.8) as a function of γ_t [26].

In the nominal SPS optics (called Q26), the phase advance per FODO cell is close to $\pi/2$, resulting in betatron tunes between 26 and 27. Low dispersion in the long straight sections is achieved setting the arc phase advance to $4\times2\pi$. In the case of the nominal SPS optics, the LHC-type proton beams are injected at 26 GeV/c (γ=27.7), i.e. above transition (γ_t=22.8). By reducing γ_t, the slippage factor is increased throughout the acceleration cycle with the largest relative gain at injection energy, as shown in Fig. 4, where η normalized to the value in the nominal SPS optics (η_{nom}) is plotted as a function of γ_t, for injection and extraction energy. Significant gain of beam stability can be expected for a relatively small reduction of γ_t, especially in the low energy part of the acceleration cycle. In 2010, alternative optics solutions for modifying γ_t of the SPS were investigated [26]. Based on the fact that in a regular FODO lattice the transition energy is approximately equal to the horizontal tune, γ_t can be lowered in the SPS by reducing the horizontal phase advance around the ring. One of the possible solutions, with low dispersion in the long straight sections, is obtained by reducing the arc phase advance by 2π, i.e. μ_x, $\mu_y \approx 3\times2\pi$ so that the machine tunes are close to 20 (“Q20 optics”). In this case, the transition energy is lowered from γ_t = 22.8 in the nominal optics to γ_t = 18 and η is increased by a factor 2.85 at injection and 1.6 at extraction energy (Fig. 4). Note that the maximum β-function values are about the same in both optics, whereas the minima are increased by about 50%. The optics modification is mostly affecting peak dispersion, which is almost doubled. The fractional tunes have been chosen identical to the nominal optics in order to allow for direct comparison in experimental studies. A series of measurements with high-intensity single bunches were conducted during the last years [27, 28], in order to quantify the benefit of the Q20 optics with respect to TMCI. In the nominal optics, the threshold with nominal longitudinal emittance and close to zero chromaticity is found at 1.6×10^{11} p/b, as shown in Fig. 5 (left). In order to

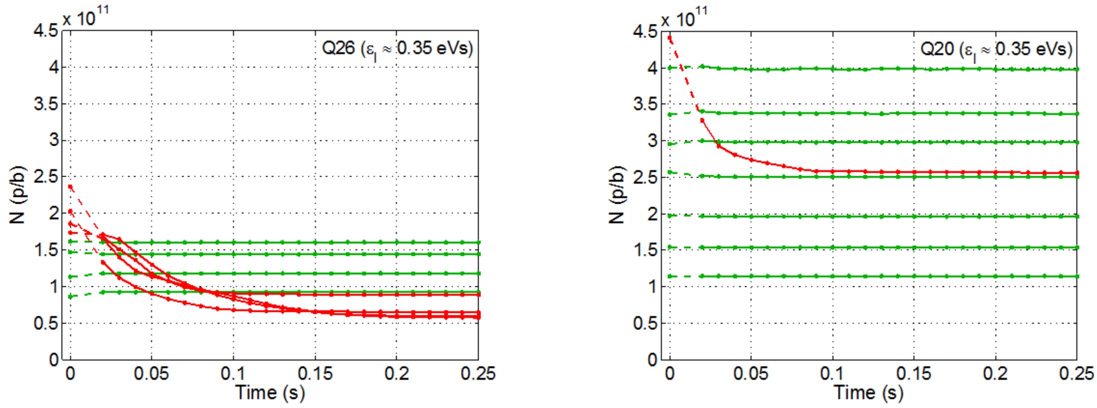

Figure 5: Examples of the intensity evolution as a function of time after injection in the Q26 optics (left) and the Q20 optics (right). Green curves correspond to stable beam conditions, red traces indicate cases above the TMCI threshold [28].

pass this threshold with the Q26 optics, the vertical chromaticity has to be increased so much that the losses are excessive due to single-particle effects. In the Q20 optics, it was demonstrated that up to 4×10^{11} p/b could be injected with no sign of the TMCI and low chromaticity, as shown in Fig. 5 (right) [28]. Such high intensity single bunches were already sent to the LHC for beam studies [29].

The ECI threshold scales with the synchrotron tune [30]. Therefore a clear benefit from the larger η in the Q20 optics is expected. Numerical simulations were performed, assuming that the electrons are confined in bending magnets [31]. The expected threshold electron density ρ_c for the ECI instability in the nominal (red) and the Q20 optics (blue), as a function of the bunch intensity N_b at injection energy, for matched RF voltages, is presented in Fig. 6. Clearly, higher thresholds are predicted for Q20.

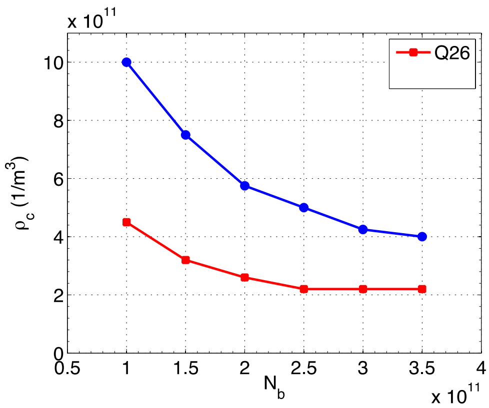

Figure 6: ECI thresholds for various intensities comparing the nominal (red) with the low γ_t SPS optics (blue) [28].

To stabilize the LHC beam at flattop in the Q26 optics from longitudinal instabilities, controlled longitudinal emittance blow-up is performed during the ramp. The maximum voltage of the 200 MHz RF system is needed in order to shorten the bunches for beam transfer to the LHC 400 MHz bucket. Due to the limited RF voltage, bunches with the same longitudinal emittance at extraction will be longer in the Q20 optics. In fact, for the same longitudinal bunch parameters of a stationary bucket, the required voltage would need to be scaled with η. However, the longitudinal instability threshold at 450 GeV/c is about 50%

higher in the Q20 optics and therefore less or no controlled longitudinal emittance blow-up is required compared to the nominal optics, for achieving the same beam stability. Figure 7 shows a comparison of the beam stability (bunch length and bunch position) in the two optics, for a single 50 ns LHC batch with 1.6×10^{11} p/b. The Q20 optics is stable even in the absence of emittance blow-up, with a mean bunch length of around τ=1.45 ns at flattop, which is compatible with injection into the LHC.

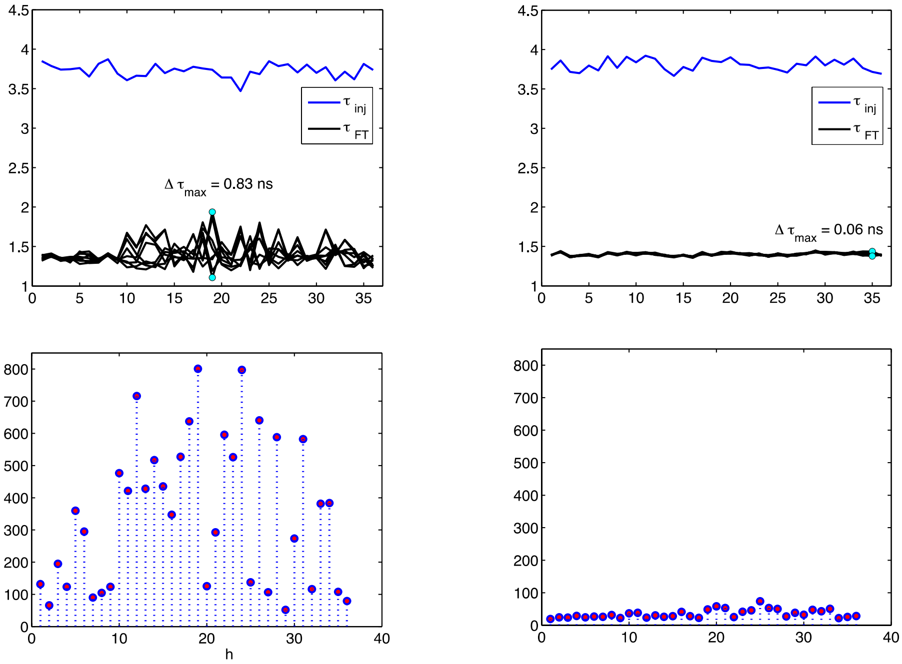

Figure 7: Bunch length (top) and bunch position oscillations (bottom), at flattop, for a single batch 50 ns LHC beam, for Q26 (left) and for Q20 (right) [27].

The low transition energy optics in the SPS became operational on September 2012. The switch to this new optics was very smooth, allowing very high brightness beams to be delivered to the LHC providing record luminosities [29]. This optics opens the way for ultra-high brightness beams to be delivered in the HL-LHC era for protons and eventually for ions [32].

2.26.6 **Summary**

Using analytical and numerical methods, linear optics parameters, which have a direct impact on collective effects, were optimized for specific examples of high-intensity, high brightness, hadron and lepton rings. These approaches allowed a solid conceptual design of ultra-low emittance damping rings and permitted to break intensity limitations in an existing LHC injector, without any cost impact or hardware change. It is certain that there is a growing need for the optics designer to transcend the single-particle dynamics mentality and apply such optimization procedures for reaching the optimal performance of rings, in design or operation.

2.26.7 **References**

1. A. W. Chao, Physics of Collective Beam Instabilities in High Energy Accelerators, New York, Wiley (1993).
2. T. Argyropoulos et al., TUPWA040, IPAC13 (2013).
3. W. Höfle, FRXCA01, IPAC13 (2013).
4. P. Collier et al., EPAC02, WEPRI082, p.1458 (2002).
5. G. Rumolo, et al., PRL100, 144801 (2008).
6. L. J. Laslett, BNL-7534 (1963).
7. A. Piwinski, in Handbook of Accelerator Physics ed. A. W. Chao, M. Tigner, World Scientific, p. 127, 2002; J. Bjorken, S. K. Mtingwa, Part. Accel. 13, 115 (1983).
8. J.Wei, in Handbook of Accelerator Physics, op. cit., p.285.
9. T. Risselada, 4th CAS, CERN-91-04, p.161 (1991).
10. K. Y. Ng, in Handbook of Accelerator Physics, op. cit., p. 94.
11. S. Y. Lee, K. Y. Ng, D. Trbojevic, PRE, 48(4), p. 3040 (1993).
12. Y. Yamazakied, KEK-2002-13 (2002).
13. Y. Papaphilippou et al., TH6PFP044, PAC09, p.3805 (2009).
14. Y. Papaphilippou et al., THPWO081, IPAC13 (2013).
15. S. Hancock, CERN-AB-Note-2006-39 (2006).
16. D. S. Robin et al., PRST-AB11, 024002 (2008).
17. H. Bartosik et al., THPE022, IPAC10 (2010).
18. Y. Papaphilippou et al., TUPPC086, IPAC12, p. 1368 (2012).
19. F. Antoniou, PhD Thesis, NTUA (2013).
20. F. Antoniou et al., WEPE085, IPAC10, p.3542 (2010).
21. K. Kubo et al., PRST-AB8, 081001 (2005).
22. H. H. Braun et al., CLIC Note 849 (2010).
23. F. Antoniou and Y. Papaphilippou, preprint (2013).
24. D. Schoerling et al., PRST-AB15, 042401 (2012).
25. LIU-SPS Beam Dynamics Working Group, chaired by E. Shaposhnikova, http://paf-spsu.web.cern.ch/paf-spsu/
26. H. Bartosik et al., MOPS012, IPAC11, p.619 (2011).
27. H. Bartosik et al., MOPS010, IPAC11, p. 613 (2011); WEPPR072, IPAC12, p. 3096 (2012).
28. H. Bartosik, PhD Thesis, TU Wien, (2013).
29. Y. Papaphilippou et al., THPWO080, IPAC13 (2013).
30. K. Ohmi and F. Zimmermann, PRL85, 3831 (2000).
31. H. Bartosik et al., MOPS011, IPAC11, p.616 (2011).
32. F. Antoniou et al., TUPME046, IPAC13 (2013).